

## NUMERICAL SIMULATION OF COMBUSTION LAB EXPERIMENTS ON WET FORWARD COMBUSTION

**Lucia Inês Bonet Gonçalves, [lucia@dep.fem.unicamp.br](mailto:lucia@dep.fem.unicamp.br)**

**Osvair Vidal Trevisan, [trevisan@dep.fem.unicamp.br](mailto:trevisan@dep.fem.unicamp.br)**

Department of Petroleum Engineering – State University of Campinas (UNICAMP)  
Caixa Postal 6122 – CEP 13083-970 – Campinas – SP - Brasil

**Abstract.** *One way to improve the performance of conventional underground combustion process (dry forward combustion) is to inject air and water either simultaneously or intermittently, named as wet forward combustion. The heat capacity of dry air is considerably lower than that of water, such that water may render a better transport of the heat generated by the combustion front, eventually leading to the reduction of the amount of air required to sweep a specified reservoir volume. Since the cost of air compression is one of the main items involved in the economic analysis of a combustion project, reduction of the air requirement is an important benefit and should be pursued. In this work, a study of the wet forward combustion was performed through numerical simulation of a combustion tube experiment with the properties of an onshore heavy oil field located at Espírito Santo state in Brazil. Input data used for the numerical model refer to previous works developed at the Department of Petroleum Engineering at State University of Campinas. A sensitivity analysis was realized for different parameters applied in the combustion tube experiment, such as water-air ratio, initial saturations, operating pressure and water-air alternation. Results showed that oil recovery increases and is anticipated with increasing water injection ratios until an optimum value is reached. After this value, oil recovery decreases, because the burning front is not sustained. Higher initial oil saturations presented higher oil recovery factors. Increasing the operating pressure resulted in better oil recovery coefficients. Water-air alternation showed a small increase in oil recovery, with lower volume of water and air, when compared to water and air co-injection. However, the final recovery is considerably postponed. The results give a good indication on the values of these parameters in order to perform future laboratory experimental tests for the crude oil studied.*

**Keywords:** *Wet Forward Combustion, Numerical Simulation, Combustion Tube Tests, Heavy Oil*

### 1. INTRODUCTION

The application of Enhanced Oil Recovery (EOR), such as thermal methods, is recommended for those reservoirs where the conventional methods of oil recovery do not provide economic efficiency or when they arrived to their economic limit.

The main objective of the thermal methods is to raise reservoir temperature to reduce oil viscosity and consequently improve oil mobility and its recovery. Many experiences were studied with the intention of providing heat to the heavy oil formation, and among them it is possible to mention in-situ combustion (Correia, 1986).

Like all other enhanced oil recovery methods, in-situ combustion involves high operational costs and, because of that, a detailed geology and engineering study of the candidate reservoirs must be performed in order to verify its technical and economic viability. Laboratory tests, field pilots and numerical simulations are among the studies to be carried out, and their results checked against each other, to provide a better performance prediction for the method.

Laboratory studies have included combustion tube tests, which can provide much useful information about combustion characteristics of the analyzed rock-fluid system. Hence, many researchers state the laboratory combustion tube studies as a mandatory requirement for the design of an in-situ combustion project (Moore *et al.*, 1994; Sarathi, 1999; Brigham and Castanier, 2007).

Numerical simulation of the combustion process offers additional complexities when compared to simulation of steam injection processes. In addition to all difficulties of simulating a thermal process, a combustion simulator must include the chemical reactions associated with the formation of coke, its oxidation, the oxidation of medium and light hydrocarbons and be able to handle large variations in saturations and temperatures. The advantage of the numerical simulation is that the effects of process variables can be studied at a substantially lower cost than a detailed laboratory experimental investigation (Kumar, 1987).

The present paper reports on the development of a simulation model for combustion tube experiments using a commercial simulator, and the results of a sensitivity analysis for different parameters, such as water-air ratio, initial saturations, operating pressure and water-air alternation. The numerical model of the combustion experiment applied the properties of an onshore heavy oil field located at Espírito Santo state in Brazil and input data referred to previous works related to this subject developed at the Department of Petroleum Engineering at State University of Campinas. The main objective is to obtain a good indication on the values of the analyzed parameters in order to perform future laboratory tests for the crude oil studied.

## 2. BACKGROUND AND THEORETICAL CONCEPTS

### 2.1. Process Description of the Wet Forward Combustion

In the conventional underground combustion process, also known as dry forward combustion, air is first injected into an injection well for a short period of time and then, the oil in the formation is ignited. Ignition is usually induced using downhole gas burners, electric heaters or through injection of a pyrophoric agent such as linseed oil or a hot fluid such as steam. Once ignited, the combustion front is sustained by a continuous flow of air and it moves through the reservoir toward the production wells.

As the combustion front moves away from the injection well, several characteristic zones are developed in the reservoir between the injector and producer. These zones, which are described in detail in Sarathi (1999), are the result of heat and mass transport and the chemical reactions that occur in a forward combustion process.

In the dry forward combustion process, much of the heat generated during burning is stored in the burned sand behind the burning front and is not used for oil displacement. The heat capacity of dry air is low and, consequently, the injected air cannot transfer heat from the burned sand as fast as it is generated. Water, on the other hand, can absorb and transport heat many times more efficiently than can air. If water is injected simultaneously with air, much of heat stored in the burned sand can be recovered and transported forward. Injection of water simultaneously or intermittently with air is commonly known as wet forward combustion. The ratio of the injected water rate to the air rate (water-air ratio, WAR) influences the velocity at which the burning front advances and the oil displacement behavior (Sarathi, 1999).

Depending on the implemented WAR, the wet forward combustion process is classified as: “incomplete” when the water injected at low rate is converted into superheated steam, “normal” when the water injected at medium rate recuperates all the heat from the burned zone or “super wet” when the water injected at high rate causes the maximum temperature at the burning front to decline. Figure 1 shows the qualitative behavior of the temperature profiles with increasing WAR.

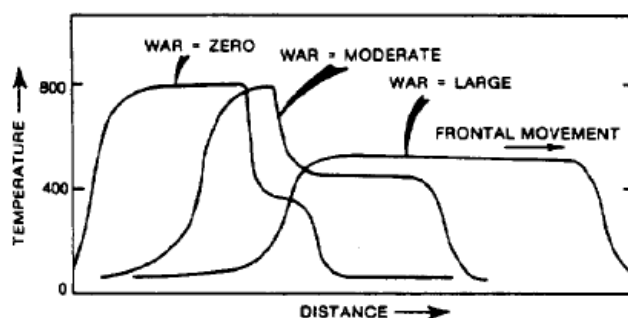


Figure 1. Qualitative temperature profile for different values of WAR (Chu, 2007).

Determining the optimum value of the WAR is a difficult task, because existing heterogeneities in the reservoir lead to different fluid saturations and flowing conditions along the burning path. When properly controlled and operated, the wet forward combustion can offer a better efficiency in the use of heat and in the oil displacement, resulting in higher recovery factors when compared to the dry forward combustion.

### 2.2. Chemical Reactions and Kinetics

The chemical reactions associated with in-situ combustion processes are complex and numerous. They occur over a broad temperature range. Most researchers group them in three classes, in ascending temperature ranges:

1. Low Temperature Oxidation (LTO) – reactions that add oxygen to the crude oil, producing water and oxygenated hydrocarbons. They generally increase original oil viscosity, boiling range, density and fuel deposition, factors that decrease oil mobility and promote high air requirement;
2. Medium Temperature Reactions – reactions of pyrolysis or thermal cracking of hydrocarbons, key for fuel (coke) production;
3. High Temperature Oxidation (HTO) – reactions by which the fuel interacts with oxygen to form water and carbon oxides. The heat generated from these reactions provides the thermal energy to sustain and propagate the combustion front.

The kinetics of the combustion reactions can be defined as the study of the chemical reactions rate and how much of the oil is affected. It characterizes oil reactivity, determines ignition conditions and provides kinetics parameters as input for possible numerical simulation of the process (Brigham and Castanier, 2007).

As crude oils contain hundreds of different compounds, it is impossible to accurately represent all the reactions occurring during an in-situ combustion process. Even if it were possible, the use of such information in numerical

models would be unfeasible due to cost and computer limitations. Based on this, most studies use a simplified model based on the Arrhenius reaction expressions defined as:

$$R_c = \frac{dC_f}{dt} = K p_{O_2}^a C_f^b \quad (1)$$

where  $R_c$  is the reaction rate of the crude oil,  $C_f$  is the concentration of fuel,  $p_{O_2}$  is the oxygen partial pressure,  $K$  is the reaction rate constant and the exponent constants  $a$  and  $b$  are the orders of the reactions with respect to oxygen partial pressure and fuel concentration respectively.

$$K = A \exp(-E/RT) \quad (2)$$

where  $A$  is the Arrhenius constant,  $E$  is the activation energy,  $T$  is the absolute temperature and  $R$  is the universal gas constant.

A variety of experimental techniques can be used to determine kinetic parameters, but it is expensive and reported literature values are often used for simulation work (Sarathi, 1999).

### 2.3. Particularity of the Combustion Simulation

Specifically for in-situ combustion modeling, the thermal simulator must describe the chemical reactions that occur during the process. There are two types of in-situ combustion models: *reactant-controlled* model where oxygen is assumed to react instantaneously with oil on contact and *kinetic-controlled* model where the rates of oil oxidation and all other reactions that may be considered can be defined by Arrhenius rate expressions.

The *kinetic-controlled* model is adequate for simulation of laboratory-scale experiments, but it is less satisfactory for solving field-scale problems. The energy released by oxidation is spread over the relatively large gridblocks used in a field-scale model, which results in an unrealistically small rise in the temperature. Depending on the activation energies used in the Arrhenius rate expressions, the computed temperatures may not be high enough to sustain reaction at a reasonable rate (Mattax, 1990).

## 3. METHODS AND PROCEDURES

The simulation model was based on the combustion tube set-up of the Department of Petroleum Engineering at Unicamp which was designed for this purpose. The schematic of the apparatus is shown in Fig. 2. The tube is made of stainless steel with an external diameter of 7,68cm, an internal diameter of 6,93cm and length of 100cm. At the top flange there is a connection for air and water injections and at the bottom flange there is a connection for production of the fluids which pass through a two-stage separation in order to be segregated in oil, water and gas phases.

The tube is packed with a homogeneous mixture of sand, clay, water and oil. The tips (around 1cm length) of the tube were packed with clean thicker sand in order to help the fluid distribution and to avoid flow blocking. Ignition is obtained with a external electric heater, which furnishes heat to the first 10cm of the tube. A detailed explanation of the apparatus and experimental procedures can be found in Chicuta (2008).

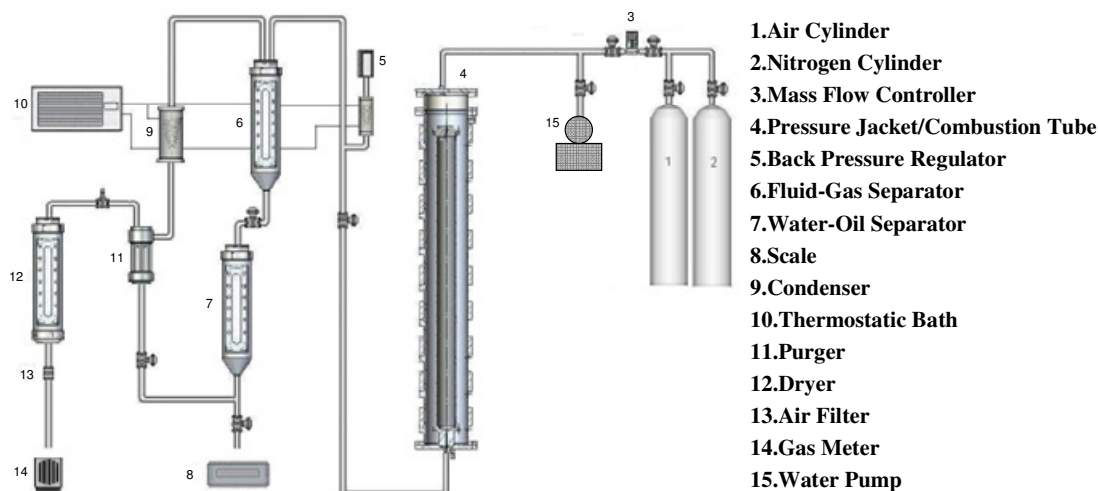


Figure 2. Combustion tube set-up of the Department of Petroleum Engineering at Unicamp (Chicuta, 2008).

### 3.1. Simulator

The study was developed using the commercial simulation software STARS (Steam, Thermal and Advanced Process Reservoir Simulator) 2007.10 version developed by CMG (Computer Modeling Group Ltda.). The simulator allows for four phases (oil, water, gas and solid fuel). It rigorously models all the important physical and chemical processes taking place during the in-situ combustion process.

### 3.2. Simulation Grid

The physical model was represented in cylindrical coordinates by a radial grid 4x1x100 (total of 400 cells). At the IJ (r,θ) plane, the area referring to the sandpack is refined into three concentric cells and the thin area referring to the metal tube is not refined. There was no refinement in the angular direction since the model simulates a linear flow. The injector and producer wells were perforated in cells 1,1,1 and 1,1,100 respectively. The grid system is schematically shown in Fig. 3.

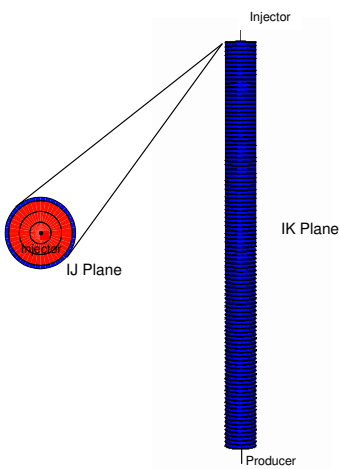


Figure 3. Grid System.

Table 1 – Reservoir Properties.

Initial Temperature	51 °C
Porosity	36 %
Absolute Permeability	9.87e-6 μm <sup>2</sup>
Rock Heat Capacity	2.35e+06 J/m <sup>3</sup> -°C
Rock Thermal Conductivity	6.23e+03 J/m-hr-°C

Table 2 – Initial Parameters Applied to the Studied Scenarios.

Case no.	CASE1	CASE2	CASE3	CASE4	CASE5	CASE6
Op. Pressure, kPag	1,034	1,034	1,034	1,034	1,034	2,068
Initial So, %	50	65	35	65	35	50
Initial Sw, %	25	25	25	10	40	25
Initial Sg, %	25	10	40	25	25	25

### 3.3. Reservoir Properties

The properties of the sandpack are given in Tab. 1. A higher permeability value, of 9.87e-03 μm<sup>2</sup>, was assigned to the tips of the tube, represented by the grid blocks 1:3,1,1 and 1:3,1,100, to model the more permeable sand layers.

The thermal properties were obtained from typical values informed by STARS (2007) and they were applied to the entire grid system, including the tube region. A previous study (Kumar, 1987) showed that the rock thermal conductivity did not influence the combustion front temperature neither its velocity.

The initial saturations and the operating pressure were some of the parameters used to perform the sensitivity analysis. They are shown in Tab. 2, listed according to the studied scenarios.

The relative permeability curves, shown in Figures 4(a) and 4(b), were based on analytical curves with exponents of 2.0, as seen in the literature (Coats, 1980). The capillary pressure was assumed as negligible.

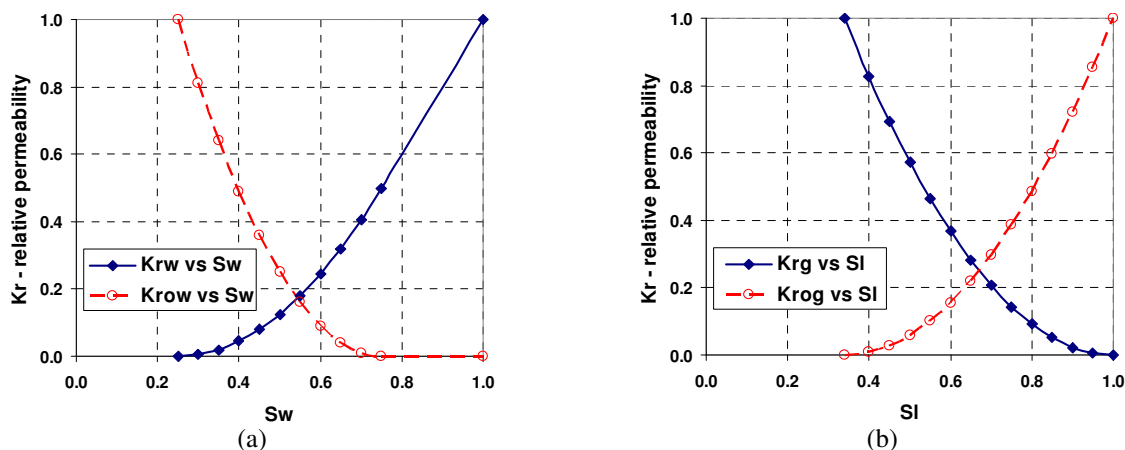


Figure 4. (a) Water-Oil Relative Permeability Curve. (b) Gas-Liquid Relative Permeability Curve.

### 3.4. Fluid Properties

The dead oil used in this study was subdivided into two pseudocomponents: a medium oil pseudocomponent (C6-C29) with a molecular weight of 254.2 and a heavy oil pseudocomponent (C30-C44) with a molecular weight of 781.3. For the experimental conditions, the pseudocomponent C30-C44 was considered only in the oleic phase, the pseudocomponent C6-C29 was considered initially in the oleic phase, but during experiment could also be in the gaseous phase.

The original viscosity curves were provided by PETROBRÁS, but extrapolation was necessary to cover low temperatures. Since the water injection is performed at temperatures as low as of 21 °C, the top region of the tube cools much faster than in dry forward combustion experiments. The extrapolation was performed using scientific software Origin 6.1 and the correlations used are given in Equations (3) and (4). Figures 5(a) and 5(b) show the oil viscosity curves. A more detailed explanation of the fluid characterization can be found in Pereira (2008) and Blaitterman (2008).

$$\text{C6-C29: } \mu = (16478.28 \times \exp(-T/15.18) + 296696.34 \times \exp(-T/6.74))/1000 \quad (3)$$

$$\text{C30-C44: } \mu = (5022420 \times \exp(-T/6.14) + 111592.28 \times \exp(-T/15.83))/1000 \quad (4)$$

where  $\mu$  is the dynamic viscosity (Pa.s) and T is the temperature (°C).

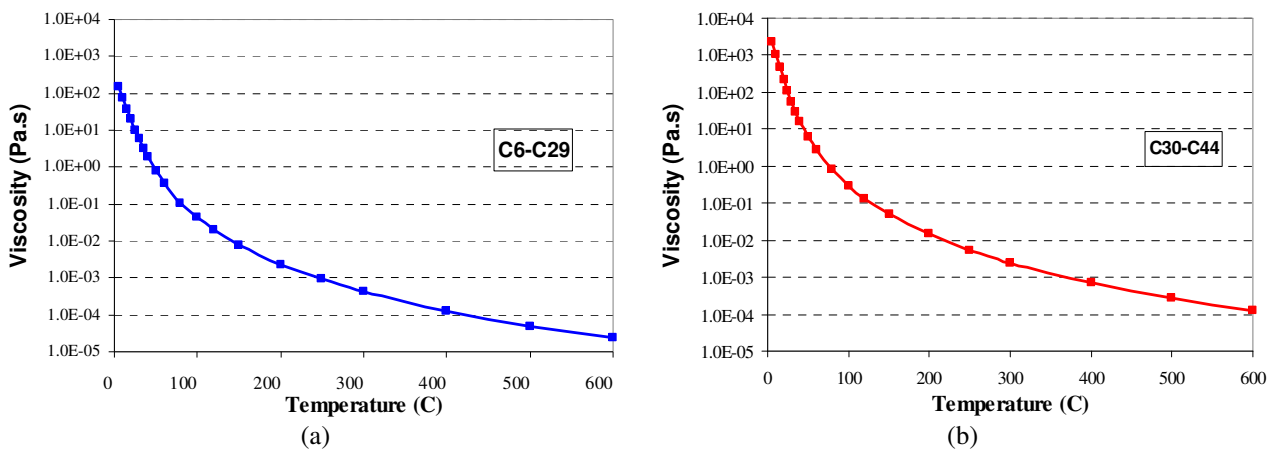


Figure 5. (a) C6-C29 Viscosity Curve. (b) C30-C44 Viscosity Curve.

The fluid model is composed of seven components: CO<sub>2</sub>, N<sub>2</sub>, O<sub>2</sub>, H<sub>2</sub>O, C6-C29, C30-C44 and COKE. COKE component was considered to be only in solid phase.

Air (79% N<sub>2</sub> and 21% O<sub>2</sub>) injection is performed at a standard constant rate of 0.18m<sup>3</sup>/h for all scenarios, while the water (100% H<sub>2</sub>O) injection rate varies to represent different water-air ratios.

### 3.5. Reaction Model

The simulation model considered the kinetic-controlled reaction model. Four chemical reactions, based on STARS sample “sttst01.dat”, were adopted in the reactions model. This included one cracking reaction and three HTO combustion reactions. The stoichiometry of the reactions is shown in Tab. 3.

Table 3 – Chemical Reactions Adopted in the Simulation Model.

Cracking:	$1.12HOIL \rightarrow 1.721MOIL + 33.4COKE$
Medium Oil Oxidation:	$1.00MOIL + 22.6O_2 \rightarrow 18H_2O + 15CO_2$
Heavy Oil Oxidation:	$1.00HOIL + 9.8O_2 \rightarrow 9.5H_2O + 21CO_2$
Coke Oxidation:	$1.00COKE + 1.18O_2 \rightarrow 0.5H_2O + 0.95CO_2$

The reaction rates followed Arrhenius equations and the specific values for the kinetic parameters are shown in Tab. 4.

Table 4 – Kinetic Parameters.

Reaction	Arrhenius Constant ( $hr^{-1}kPa^{-1}$ )	Activation Energy (J/g-mole)	Enthalpy (J/g-mole)
Cracking	6.05e+04	2.28e+07	0
Heavy Oil Oxidation	4.38e+09	5.02e+07	3.07+09
Medium Oil Oxidation	4.38e+09	5.02e+07	1.32+10
Coke Oxidation	6.05e+04	2.13e+07	2.37e+08

### 3.6. Well Model

The modeling of the production and injection wells was based on STARS sample “sttst02.dat”. The main feature is the perforation model classified as *tube-end*, in which the *well-index* parameter is calculated based on a linear flow instead of a radial flow. This model is appropriate for the end of a core face, such as found in laboratory core experiments. The geometry adopted a radius of 0.5mm, complete circumference and no *skin* factor.

## 4. RESULTS AND DISCUSSIONS

### 4.1. Water-Air Ratio

One of the main parameters to be established in a wet combustion tube test is the quantity of water to be injected associated with the quantity of injected air, known as water-air ratio (WAR). In many cases, the amount of water added is about 200 to 250 bbl per million SCF of air (i.e. 1,120 to 1,400 m<sup>3</sup>/MMm<sup>3</sup>) (Butler, 1991).

The choice of the WAR to be employed has been discussed by Chiu (1989). Based on his study, the minimum water-air ratio required for water to be available for evaporation can be estimated from Eq. (5). It assumes that, at the limit, water occupies 80% of the porous volume behind the front.

$$R_{wa} = \frac{0.8 \times \phi \times \rho_w \times B_g}{B_g \times R_{ar} + 0.2 \times \phi} \quad (5)$$

where  $R_{wa}$  is the mass of water per unit volume of air,  $R_{ar}$  is the volume of air required to burn a unit volume of reservoir,  $\phi$  is the porosity,  $B_g$  is the formation volume factor of the air behind the front and  $\rho_w$  is the specific mass of water.

Considering  $\phi = 0.36$ ,  $\rho_w = 1 \text{ g/cm}^3$ ,  $B_g \sim 0.1$  ( $\sim 1/10\text{atm}$ ),  $R_{ar} = 296.6 \text{ m}^3/\text{m}^3$  (Chicuta, 2008), the following result is obtained:  $R_{wa} \sim 9.7\text{e-}04 \text{ g/cm}^3 \sim 971 \text{ m}^3/\text{MMm}^3$ . For the base model CASE1 with a constant air injection of 0.18m<sup>3</sup>/h, the WAR was varied between 0 and 2,807 m<sup>3</sup>/MMm<sup>3</sup> (i.e. water injection rate from 0m<sup>3</sup>/min to 5e-04m<sup>3</sup>/h), with discrete values of 0; 281; 561; 842; 954; 1,123; 1,684; 2,246 and 2,807 m<sup>3</sup>/MMm<sup>3</sup>.

Also, in addition to WAR variation, the start time of water injection was varied. The literature shows different criteria for the start time to water injection in combustion tube experiments. White and Moss (1983) described as mandatory obtaining stable tube operating conditions to start water injection, which usually occurs when the burning front reaches 25-50% of the tube length. In the results published by Bagci (2006), water injection started when the burning front was observed at the second and third thermocouples. In the simulation results published by Kumar (1987), water injection started when the combustion front had propagated to the second grid block or 16% of the tube length.

For the base model CASE1 with WAR=0, the combustion process started after 0.65h of simulated experiment, when the ignition temperature of 500 °C was reached. The burning front was observed at the positions of 5cm after 1h, of 15cm after 1.8h and of 45cm after 2.6h. Based on this, start time of water injection was varied between 1h and 2.5h.

The results of WAR and start time of water injection variation effects on oil recovery factor and maximum temperature for the base model CASE1 can be verified in Figures 6(a) and 6(b), respectively.

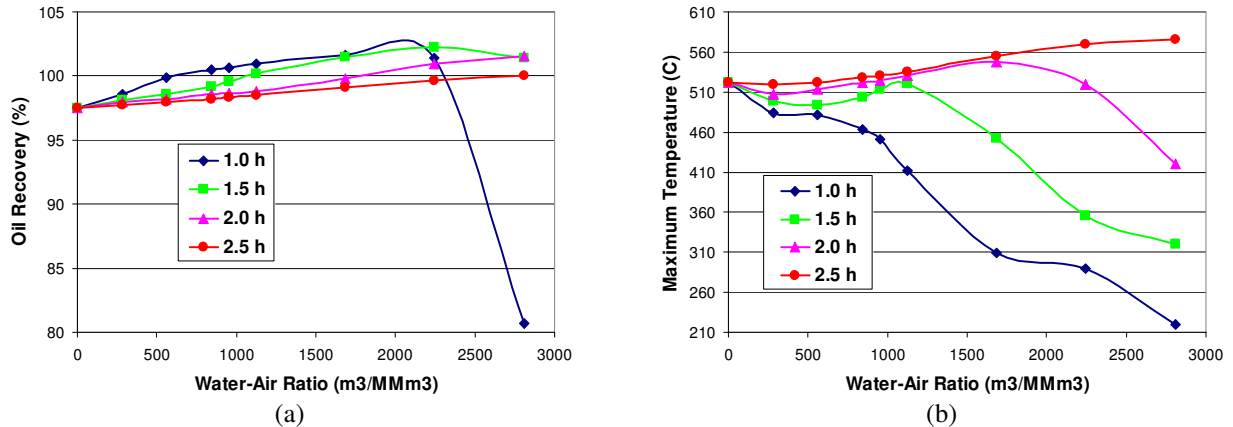


Figure 6. Effects of WAR and start time of water injection on oil recovery factor (a) and on maximum temperature (b).

The oil recovery factor increases with increasing WAR until an optimum value. After such value, oil recovery decreases with increasing WAR. Bagci (2006) observed that same behavior. The variation of the start time of water injection shows that the sooner it occurs, the higher is the oil recovery factor and the smaller is the optimum WAR.

Regarding the effects on the maximum temperature, no trend is observed. There are increases and decreases in the maximum temperature with increasing WAR. It can be attributed to two opposite effects resulting from the extended steam and condensing zones ahead of the combustion front: 1) rock and fluids are preheated before the combustion front reaches them, which tends to increase the temperature of the front; 2) steam reduces the concentration of residual oil remaining in the path of the advancing combustion front, which substantially reduces the fuel concentration and tends to lower temperature of the front. Regarding the variation of the water injection start time, it shows that the sooner water is injected the lower is the maximum temperature reached by the combustion front.

Temperature profiles along the tube, shown in Fig. 7, present stable rates of advance of the combustion front for different water-air ratios and faster movement with the increasing WAR. Also, it is worth pointing to the lowering in the temperature profile behind the combustion front and to the extending of the steam plateau ahead of the front.

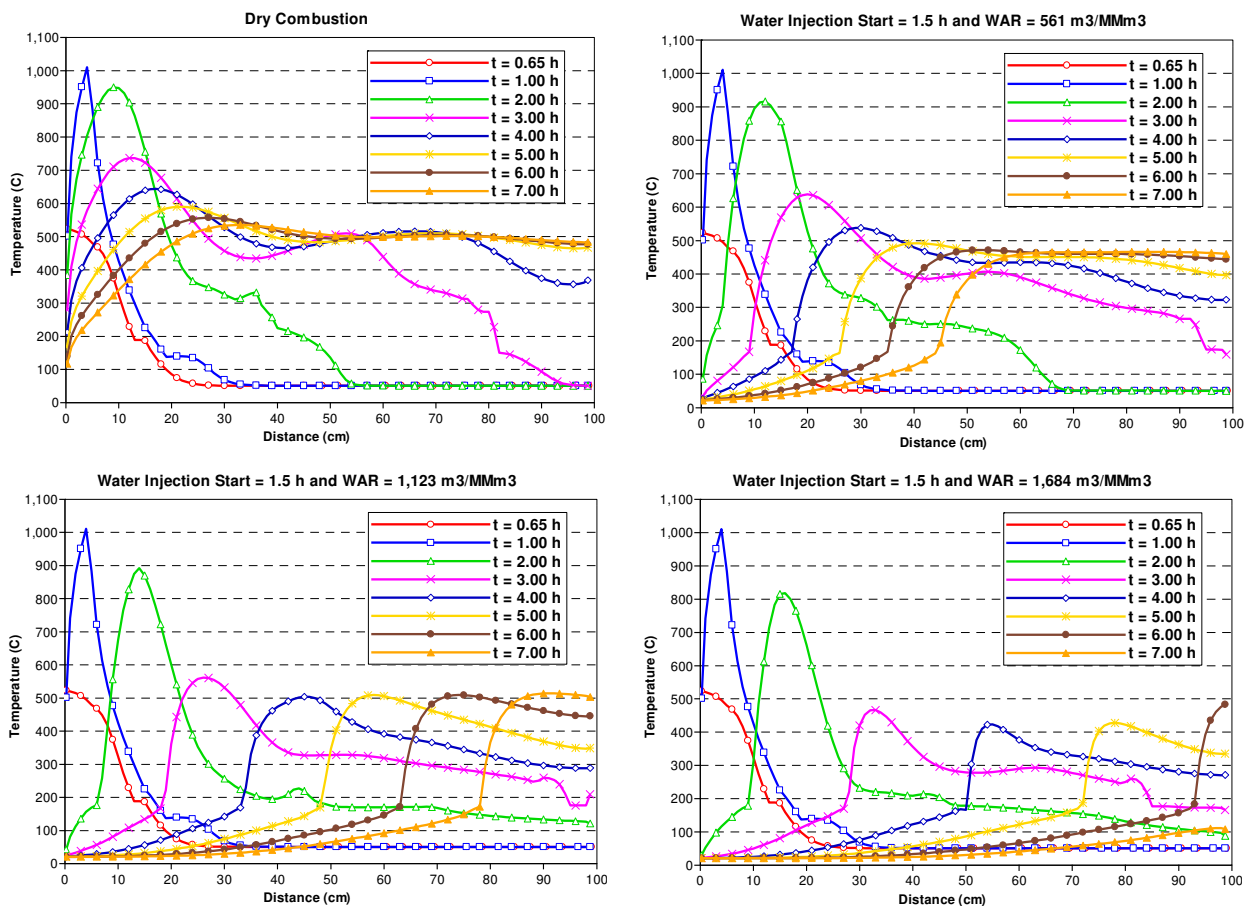


Figure 7. Temperature profile for different water-air ratios.

The increase in the advance rate of the combustion front reflects on the time for the ultimate oil recovery, which can be observed in Fig. 8. The final recovery is reached sooner with increasing WAR. For the WAR of 1,684 m<sup>3</sup>/MMm<sup>3</sup>, the ultimate recovery factor is higher but not anticipated. Based on these results, the base model CASE1 with WAR of 1,123 m<sup>3</sup>/MMm<sup>3</sup> (i.e. water injection rate of 2e-04m<sup>3</sup>/h) and water injection start at 1.5h was chosen to proceed with the sensitivity analysis for the other parameters.

The volumetric oil recovery factors above 100% can be explained by the cracking reaction used in the combustion simulation model. Since this type of reaction consumes heavy oil fractions to generate medium oil and coke, the mass composition of the oil changes during the combustion process, increasing the production of medium fractions. Figure 9 shows the mass composition of the oil at the beginning of the process and for the produced oil, for the chosen scenario.

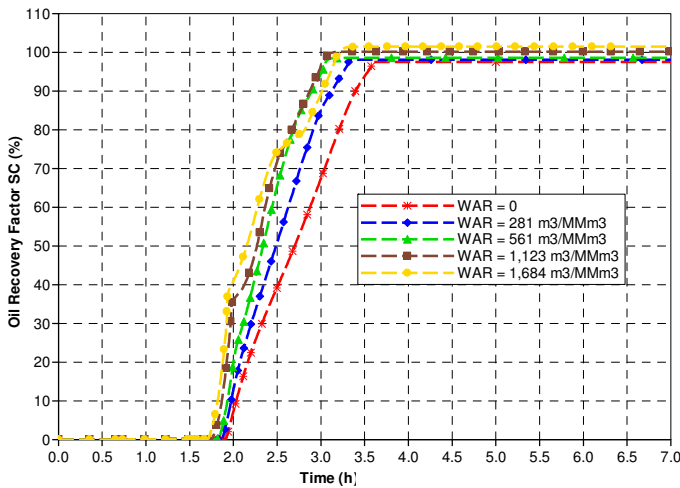


Figure 8. Oil recovery factor for different water-air ratios.

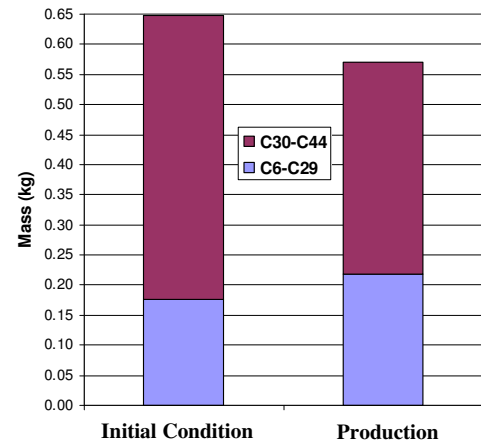


Figure 9. Oil Mass Composition.

#### 4.2. Saturations

Oil, gas and water saturations were varied to generate four additional scenarios, as described in the methods and procedures section. Keeping the start time of water injection at 1.5h, WAR was varied at the same discrete values already described. The effects on the oil recovery factor can be verified in Fig. 10. The already observed behavior of increasing the oil recovery factor with an increasing WAR until an optimum value is maintained for CASE2, 3 and 4. The overall result observed was that higher oil saturations provide higher oil recoveries.

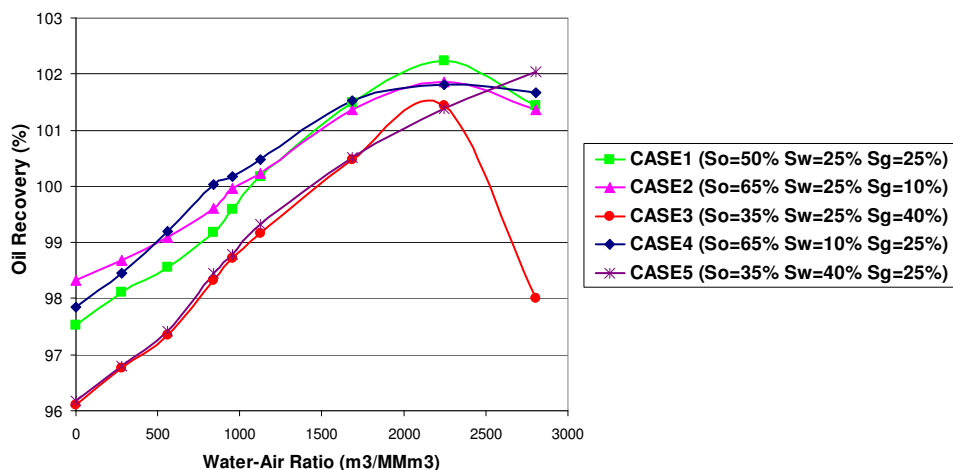


Figure 10. Effects of WAR and saturations on the oil recovery factor.

#### 4.3. Operating Pressure

Changing the operating pressure from 1,034kPa to 2,068kPa for the chosen scenario resulted in an increase of the combustion front velocity, as shown in Fig. 11.

Such effect can be explained by the variation of the gas volume. The air injection rate in reservoir conditions turns to a smaller rate when the operating pressure is increased. As for the water injection rate in reservoir conditions there is



no relevant change with the operating pressure increase. So, it will reflect in a doubled WAR, which will provide an increase in the rate of advance of the combustion front. However, the drawback of this scenario is that the lab experiment will have to face higher pressures, specially the injection pressure when starting water injection.

The same reasoning takes to a different result in the case of a dry forward combustion process. Since there is no water in this process, the increase of the operating pressure takes to a discrete decrease in the rate of advance of the combustion front. Figure 12 shows the effect for the oil recovery factor.

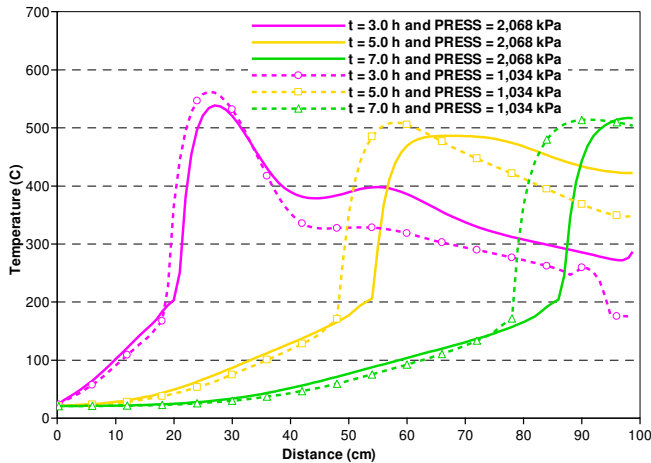


Figure 11. Effect of operating pressure increase on Temperature profile.

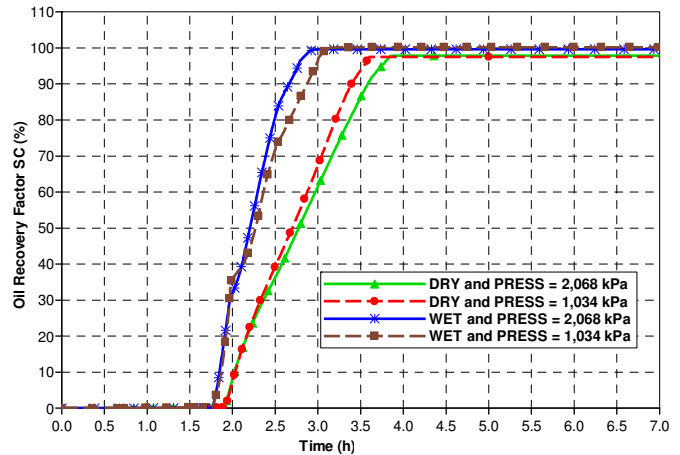


Figure 12. Effect of the operating pressure increase on oil recovery factor.

#### 4.4. Water-Air Alternation

Although the alternation of air and water injection is mentioned in the literature as an option for the wet forward combustion process, no simulation or experimental work using such configuration was found in the open literature. A scheme of 0.25h alternation between water and air injection was adopted for the chosen scenario CASE1, with water injection starting after 1.5h of simulated experiment.

Figures 13(a) and 13(b) show injection and production data in terms of volume for both injection schemes.

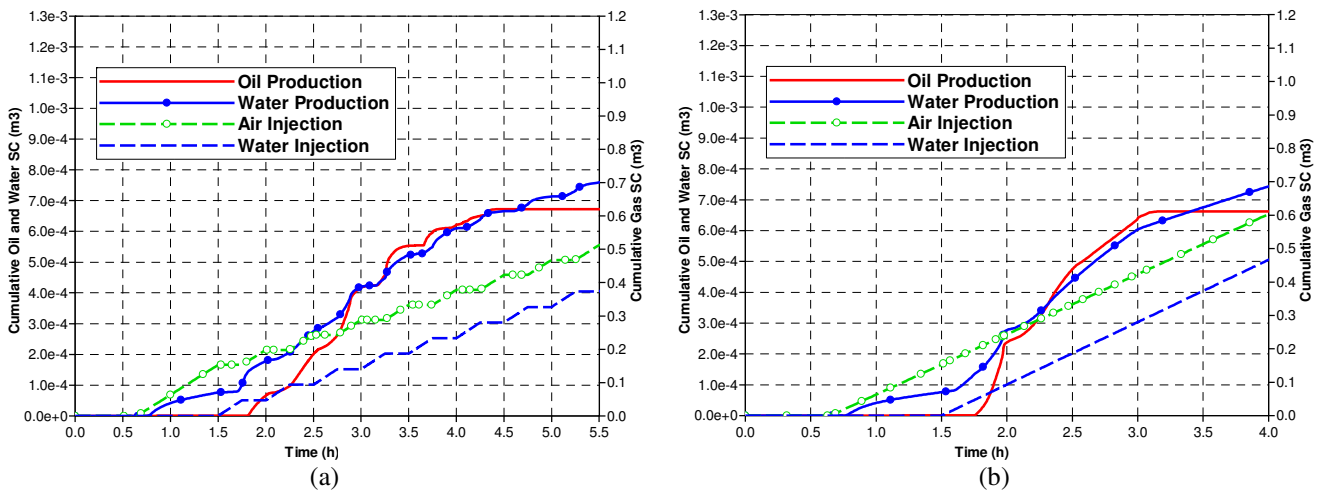


Figure 13. Injection and production data for the alternation scheme (a) and the co-injection scheme (b).

The alternation of air and water resulted in a small increase in the oil recovery (1.5%), expending practically 20% less of air and water volumes when compared to the co-injection of air and water. However, the final recovery was considerably postponed (5.3h for alternation and 4h for co-injection). A detailed economical analysis would be needed in order to compare the performance of the two options, but such analysis is beyond the scope of the present paper.

#### 5. CONCLUSIONS

The conclusions arising from the results are summarized as:

1. The combustion front velocity increases with increasing water injection ratios. Consequently, the oil recovery increases and is anticipated, reducing air consumption. This behavior is maintained until an optimum value of WAR is reached. After such value, oil recovery decreases with further increase in water-air ratio, because combustion is not sustained.
2. Regarding peak temperatures, they do not follow a continuous trend with increasing water injection ratios. The results show that for some scenarios the preheating of the rock by the extended steam zone prevails while for other scenarios the reduction in fuel concentration is the prevalent phenomenon.
3. The sooner the water injection starts, the higher is the oil recovery obtained, the lower is the optimum WAR value and the lower is the peak temperature. Based on this, among the simulated scenarios, CASE1 with a co-injection WAR of 1,123 m<sup>3</sup>/MMm<sup>3</sup> and water injection starting at 1.5 h showed the most cost-effective results and was chosen to proceed with the sensitivity analysis for other parameters. It yielded a high and anticipated oil recovery factor (100.18%) with a small reduction in peak temperature (520.82 °C).
4. For the chosen scenario, the sensitivity analysis for the initial saturations showed that scenarios with higher oil saturations ( $S_{oi} \geq 50\%$ ) resulted in higher oil recoveries.
5. For the chosen scenario, increasing the operating pressure from 1,034kPa to 2,068kPa resulted in better oil recovery factors. The combustion front velocity increases, anticipating the final oil recovery.
6. For the chosen scenario, the alternated injection of air and water resulted in a small increase in the oil recovery factor with lower volume of air and water. However the final oil recovery was considerably postponed when compared to the co-injection of air and water scenario.

## 6. ACKNOWLEDGEMENTS

The authors acknowledge Prof. Euclides José Bonet for all his helpful suggestions, Mr. Washington Botine for his support in the lab work and Finep/CTpetro and Petrobrás for the financial support.

## 7. REFERENCES

- Bagci, A.S., 2006, "Wet Forward Combustion for Heavy Oil Recovery", *Energy Sources, Part A*, 28:221-232.
- Blaitterman, G., 2008, "Simulação Computacional de Combustão In-Situ em Escala Laboratorial", Trabalho de Graduação em Engenharia Mecânica, Faculdade de Engenharia Mecânica, UNICAMP, Campinas.
- Brigham, W.E. and Castanier, L., 2007, "In-Situ Combustion", *Petroleum Engineering Handbook, Reservoir Engineering and Petrophysics, Vol. V(B)*, Society of Petroleum Engineers.
- Butler, R.M., 1991, "Thermal Recovery of Oil & Bitumen", Department of Chemical and Petroleum Engineering, University of Calgary, Prentice Hall, Alberta.
- Chicuta, A.M., 2008, "Estudo Experimental Sobre a Recuperação de Óleo Pesado da Bacia do Espírito Santo Através da Combustão In-Situ", Texto de Apoio ao Exame de Qualificação de Mestrado em Ciências e Engenharia de Petróleo, Faculdade de Engenharia Mecânica, UNICAMP, Campinas.
- Chiu, K.W., 1989, "Analytical Analysis of Air/Oxygen Wet Combustion by Energy Balance", The fourth UNITAR/UNDP International Conference on Heavy Crude and Tar Sands. Vol 4: In Situ Recovery, AOSTRA, Edmonton, pp. 807-825.
- Chu, C., 2007, "Thermal Recovery", *Petroleum Engineers Handbook, Part 5, Chapter 46*.
- Coats, K.H., 1980, "In-Situ Combustion Model", SPEJ 533-54, Trans., AIME, 269.
- Correia, A.B., 1986, "Avaliação do Projeto Piloto de Combustão In-Situ de Carmópolis", Dissertação de Mestrado em Engenharia de Petróleo, Escola de Minas, Universidade Federal de Ouro Preto, Ouro Preto.
- Kumar, M., 1987, "Simulation of Laboratory In-Situ Combustion Data and Effect of Process Variations", SPE 16027.
- Mattax, C.C., 1990, "Reservoir Simulation", Society of Petroleum Engineers, Richardson.
- Moore, R.G., Lareshen, C.J., Belgrave, J.D.M., Ursenbach, M.G., Mehta, S.A., 1994, "In-Situ Combustion: New Ideas for an Old Process", 11<sup>th</sup> Annual Canadian Heavy Oil and Oil Sands Symposium, Calgary, Alberta.
- Pereira, A.N., 2008, "Estudo Termoanalítico e Cinético da Combustão de Óleo Pesado", Dissertação de Mestrado em Ciências e Engenharia de Petróleo, Faculdade de Engenharia Mecânica, UNICAMP, Campinas.
- Sarathi, P., 1999, "In-Situ Combustion Principles and Practices", U.S. Department of Energy, Oklahoma, Tulsa.
- STARS, 2007, Help STARS 2007.10 User's Guide, CMG.
- White, P.D. and Moss, J.T., 1983, "Thermal Recovery Methods", PennWell, Oklahoma, Tulsa.

## 5. RESPONSIBILITY NOTICE

The authors are the only responsible for the printed material included in this paper.